Inhibitory activity of the peptides derived from buffalo prolactin on angiogenesis

JAEOK LEE[1], SYAMANTAK MAJUMDER[2], SUVRO CHATTERJEE[2] and KAMBADUR MURALIDHAR[1,*]

[1]*Hormone Research Laboratory, Department of Zoology, University of Delhi, Delhi, India*

[2]*AU-KBC Research Centre, MIT Campus, Anna University, Chennai, India*

**Corresponding author (Fax, +91-11-2766-6564; Email, kambadur@hotmail.com)*

The peptide fragments obtained by cathepsin digestion of purified buffalo prolactin (buPRL) monomer have been characterized using SDS-PAGE and FPLC with regard to size and pI. Their antiangiogenic activity was tested in chick embryo chorioallantoic membrane (CAM) assay and the human endothelial cells wound healing assay. Antiangiogenic activity was observed in cathepsin-cleaved fragments from buPRL. Further, a peptide sequence 45A-46Q-47G-48K-49G-50F-51I-52T-53M-54A-55L-56N-57S-58C, which matched with human somatostatin (hSST), a known antiangiogenic factor, was located in the second loop between the first and second α-helices in the three-dimensional structure of buPRL, obtained by homology modelling. The synthetic peptide matching with SST sequence was found to exhibit antiangiogenic activity in both *in vitro* and *ex vivo* assays. It was also observed that all the peptides related to buPRL could antagonize the vascular endothelial growth factor (VEGF) and bradykinin (BK)-dependent production of endothelial nitric oxide (NO), which is a pre-requisite for endothelial tube formation. It is concluded therefore that an internal sequence in buPRL and peptide fragments derived from cathepsin-digested buPRL exhibit antiangiogenic activities.

[Lee J, Majumder S, Chatterjee S and Muralidhar K 2011 Inhibitory activity of the peptides derived from buffalo prolactin on angiogenesis. *J. Biosci*. **36** 341–354] **DOI** 10.1007/s12038-011-9073-6

1. Introduction

An isoform of rat pituitary prolactin (PRL) with intact disulfide bonds but with a nick in the sequence was discovered in 1980 (Mittra 1980a, b). This form had also been found in mouse pituitary (Sinha and Gilligan 1984), human pituitary and plasma (Sinha *et al.* 1985), and also in rat serum (Nicoll 1997). The nicked rat pituitary PRL was separated into an N-terminal 16 kDa fragment (16K) and the C-terminal 8 kDa fragment (8K) by reduction of the disulfide bonds (Mittra 1980a). The work of Clapp (1987) demonstrated that only the rat PRL (rPRL) generated the 16K fragment upon incubation with lactating rat mammary gland extracts, while ovine and human PRLs were processed into a variety of low-molecular-weight forms.

It was observed that 16K had an inhibitory effect on angiogenesis, both *in vitro* and *ex vivo*, in rat (Ferrara *et al.* 1991) and in human (Clapp *et al.* 1993), whereas intact PRL had pro-angiogenic (Struman *et al.* 1999) and proliferative action on mammary carcinoma cells (Clevenger *et al.* 2003).

Keywords. Antiangiogenesis; buffalo prolactin; prolactin-derived peptide

Abbreviations used: BBBE, bovine brain basal endothelial; BK, bradykinin; buPRL, buffalo prolactin; BUVE, bovine umbilical vein endothelial; CAM, chorioallantoic membrane; CD, cathepsin D; DAF-FM, diaminofluorescein; eNOS, endothelial NOS; FGF, fibroblast growth factor; FPLC, fast-performance liquid chromatography; GH, growth hormone; HRP, horseradish peroxidase; hSST, human somatostatin; HUVE, human umbilical vein endothelial; KS, Kaposi sarcoma; NOS, NO synthase; rPRL, rat prolactin; SST, somatostatin; VEGF, vascular endothelial growth factor

Supplementary materials pertaining to this article are available on the *Journal of Biosciences* Website at *http://www.ias.ac.in/jbiosci/Jun2011/pp341-354/suppl.pdf*

Rat 16K inhibited the basal growth of capillary endothelial cells and also that stimulated by fibroblast growth factor (FGF), but intact and nicked PRL did not show any inhibitory activity (Ferrara *et al.* 1991). Nanomolar amounts of recombinant human 16K (h16K) inhibited the growth of bovine brain basal endothelial (BBBE) cells induced by basic FGF or vascular endothelial growth factor (VEGF) (Clapp *et al.* 1993). Human 16K PRL obtained by cleavage of intact PRL using rat mammary gland extracts also inhibited basic FGF-stimulated human umbilical vein endothelial (HUVE) cells proliferation (Clapp *et al.* 1993). Further, in the chick embryo choriollantoic membrane (CAM) assay, both the 16Ks inhibited capillary formation (Ferrara *et al.* 1991; Clapp *et al.* 1993).

While cathepsin D (CD) was used for generating an antiangiogenic 16K rPRL (Baldocchi *et al.* 1993; Lkhider *et al.* 2004), Khurana *et al.* (1999a, b) showed that a 16K hPRL isoform generated from the C-terminal end using thrombin did not posses the same activity. Later, Piwnica *et al.* (2006) investigated multiple N-terminal 16K-like fragments generated by CD. The N-terminal fragments inhibited thymidine uptake induced by growth factor and MAPK activation in bovine umbilical vein endothelial (BUVE) cells. They also, reported that r16K fragment could be generated by CD secreted from various mouse tissues like kidney, spleen, brain, heart and prostate, under acidic conditions (Piwnica *et al.* 2004). Our own studies on buPRL did not indicate the presence of a 16K fragment in the CD digestion mixture. Moreover, we have reported the occurrence of size isoforms in pure preparations of buPRL (Panchal and Muralidhar 2008), and there was no 16K isoform. It was therefore it was of interest to know weather naturally occurring size isoforms of buPRL and peptide fragments derived by CD digestion of buPRL have any antiangiogenic activity. Further, the intact buPRL monomer did not exhibit any pro- or antiangiogenic activity (Muralidhar and Lee, unpublished work).

Most studies about the antiangiogenic N-terminal fragment cleaved by CD, however, have been done only in the case of rat and human PRLs. Based on these observations (Mittra 1980a; Ferrara *et al.* 1991; Clapp *et al.* 1993; Piwnica *et al.* 2004), it was hypothesized that buffalo pituitary PRL can be cleaved by cathepsin, and the fragment could inhibit angiogenesis via endothelial interference. However, it was not clear which sequence in the N-terminal fragment plays a role in the antiangiogenesis. Here, we demonstrate that buPRL size isoform produced by CD and an antiangiogenic 14-amino-acid sequence in the hormone identified by BLAST as somatostatin (SST) have an inhibitory action on angiogenesis.

2. Materials and methods

Buffalo pituitary glands were obtained from a local slaughter, Delhi. Hatched eggs were collected from the Poultry Research Station, Nandanam, Chennai. EAhy926, the immortal HUVE cell line, was obtained from the Tissue Culture Facility, UNC Lineberger Comprehensive Cancer Center, USA.

BK, CD, 4-chloro-1-naphthol, pepstatin A, diaminofluorescein (DAF-FM), SST and VEGF were purchased from Sigma, St. Louis, USA. Sephacryl S-200 beads were from Pharmacia, USA. Goat anti-rabbit IgG to horseradish peroxidase (HRP) conjugate were from Bangalore Genei, India. SST-matching sequence in buPRL was commercially synthesized by Bioconcept, India. All other reagents were of analytical grade and locally procured.

2.1 *Fractionation procedures*

2.1.1 *Purification of buffalo PRL monomer:* Freshly frozen buffalo pituitary glands were homogenized in 0.15 M $(NH_4)_2SO_4$, 1 mM PMSF with a blender. The homogenate was stirred, adjusted to pH 4.0, allowed to stand for 1 h and centrifuged at 2000*g* for 30 min (Papkoff *et al.* 1965). The acid pellet was extracted in 0.25 M $(NH_4)_2SO_4$ (set to pH 5.5) and then followed the next step mentioned in Panchal and Muralidhar's procedure (Panchal and Muralidhar 2008). The precipitation of (AP)P-I 70 was repeated twice as per published procedure (Panchal and Muralidhar 2008). The final pellets, (AP)P-III 70 and (AP)P-I 90–70, were dissolved in 100 mM NH_4HCO_3, and stored lyophilized.

2.1.2 *Sephacryl S-200 gel filtration:* The final pellets dissolved in 100 mM NH_4HCO_3 were loaded onto separate column (4.52 cm × 92 cm) of Sephacryl S-200 resin equilibrated with 100 mM NH_4HCO_3. The same volume (5.7 mL) of fractions were collected at a flow rate of 33 mL/h and monitored for absorbance at 280 nm. Peak aliquots were pooled and lyophilized and then stored at −20°C.

2.2 *Analytical techniques*

2.2.1 *Protein estimation:* Lowry's method (Lowry *et al.* 1951) and Bradford's method (Bradford 1976) were performed with few modifications to estimate protein samples.

2.2.2 *SDS-PAGE and immunoblot analysis:* Protein samples were separated by 15% SDS-PAGE under reducing or non-reducing conditions (Laemmli 1970). Gels were either stained with 0.12% Coomassie blue G-250 (Candiano *et al.* 2004), or protein transferred to nitrocellulose membrane for immunoblot analysis (Towbin *et al.* 1979) with buPRL antiserum (1:1000). Antigen–antibody complexes were detected by anti-rabbit immunoglobulin conjugated to HRP using the substrate, 4-chloro-1-naphthol.

2.2.3 *Dot blot analysis:* Two to ten microliter of the unbound fraction from the fast-performance liquid chromatography (FPLC) was placed on a nitrocellulose membrane for dot blot analysis with buPRL a/s (1:1000). Antigen–antibody complexes were detected by the same method as with immunoblot analysis.

2.3 *Enzyme digestion and peptide separation*

2.3.1 *Proteolysis with CD:* Proteolysis of intact buPRL was performed using Baldocchi's method (Baldocchi *et al.* 1993). The reaction was terminated by de-salting with 1K cut-off centrifugal device (Pall Science, USA) and the mixture lyophilized.

2.3.2 *Separation of the peptides: Elution peptides:* The peptides separated by SDS-PAGE were eluted with the protocol of Harrington (Harrington 1990).

2.3.3 *Separation of the peptides: Fast-performance liquid chromatography:* Buffalo PRL peptide mixture obtained by CD was separated by anion-exchange chromatography on an UNO Q1 column (7 mm × 35 mm, 1.3 mL; Bio-Rad, USA). Five-hundred micrograms of the mixture was dissolved with 1 mL of the equilibrium buffer (pH 8.0), and injected after filtering. All buffers were 20 mM Tris (pH 8.0) with a linear gradient 0%–100% of 1 M NaCl in 60 min with a flow rate of 1 mL/min. The column was used as the stationary phase (Vogt and Freitag 1998).

2.4 *In silico study*

2.4.1 *Prediction of tertiary structure of proteins:* The protein sequences were downloaded from NCBI (*http://www.ncbi.nlm.nih.gov/RefSeq/*). The tertiary structures of protein and peptide were built with using SWISS-MODEL (Schwede *et al.* 2003) and Bhageerath (*http://www.scfbio-iitd.res.in/bhageerath*), respectively. The tertiary structure analysis and display were done with 'Swiss-PdbViewer DeepView v4.0' (Guex and Peitsch 1997) of The Swiss Institute of Bioinformatics.

2.4.2 *Sequence alignment:* Protein sequence alignment was done with 'protein tools' of Biology WorkBench 3.2 (*http://seqtool.sdsc.edu/CGI/BW.cgi*).

2.4.3 *Biochemical characterization:* Physico-chemical parameters of proteins and peptides were determined using 'Protparam (ExPASy Proteomics tools [Gasteriger *et al.* 2005]).

2.5 *Antiangiogenic activity analysis*

2.5.1 *Cell culture:* EAhy926 (Edgell *et al.* 1983), was maintained in DMEM, supplemented with 10% fetal bovine serum, penicillin (100 U/mL), and streptomycin (50 pg/mL), at 37°C/5% CO_2 (Astec, Japan).

2.5.2 *Wound healing cell migration assay:* Cell migration was observed using the wound healing method (Staton *et al.* 2004). After 12–16 h of seeding when EAhy926 cells were confluent, a cross linear wound was created by scratching the monolayer with a 1-mm-wide sterile plastic scraper. The cells were treated with protein or peptide, and incubated for 0, 4 and 8 h. Bright-field images were acquired using a Nikon CoolPix digital camera adapted to an inverted bright-field microscope with 40× magnifications. The rate of wound healing was quantified from the images using 'ImageJ' (Release Alpha 4.0 3.2 and Adobe Photoshop version 6.0.)

2.5.3 *NO estimation:* For fluorometric NO determination, EAhy926 cells cultured in 12-well plate and incubated overnight, at 37°C/5% CO_2. Before treatment with NO inducers, cells were treated with 14K and SST and incubated for 1 h. After 14K and SST treatment, NO inducers were added to treated cells and incubated further for 15 min. Cells were washed with PBS and then incubated with 300 µL of DAF-FM, the cell-nonpermeable diacetate prepared in 1× PBS containing L-arginine (1 mM) (Kojima *et al.* 1998) and incubated at 37°C/5% CO_2 for 15 min. After transferring the supernatant to a 96-well plate, DAF-2 T fluorescence was measured using a spectrofluorometer (Cary Eclipse, EL07083326) with 495 nm excitation and 515 nm emission wavelength.

2.5.4 *Tube formation:* Tube formation experiments were performed as described earlier (Madri *et al.* 1988). In brief, 24-well plates were coated with 150 µL matrigel per well (10 ng/mL, BD Biosciences) and incubated at 37°C for 30 min for gelling. EAhy926 cells (1×10^4) in 1 mL/well were seeded in the absence or presence of the synthetic peptide derived from buPRL in DMEM. After 48 h of incubation at 37°C/5%CO_2 humidified atmosphere, the centre of each well was photographed with a Nikon Coolpix camera attached to a phase contrast microscope. Tubes formed in each well were counted and plotted as a graph.

2.5.5 *CAM assay:* CAM assay was performed using fourth or sixth day incubated white leg horn eggs (Ribatti *et al.* 1996). The eggs were broken and gently plated onto dishes under sterile conditions. Disks contacting target factors including control (1× PBS) were placed on the vascular bed of egg yolks, and the yolks were incubated for 12 h. Images were taken at a 20× magnification using a Nikon CoolPix digital camera adapted to a stereo-microscope after 0, 4, 8 and 12 h of incubation. Analysis of angiogenesis was performed by using Adobe Photoshop 7.0 and 'Angio-Quant' software (Niemisto *et al.* 2005).

2.5.6 *Statistical analysis* All experiments were performed in triplicate ($n=3$) unless otherwise specified. The data are presented as means±standard error (SE). The data were analysed using a one-way ANOVA test as appropriate (Sigma Stat software). $P \leq 0.05$ was considered statistically significant.

3. Results

3.1 *Purification of enzyme-free buffalo prolactin monomer*

Highly pure buPRL monomer was obtained from pituitary glands with the modified Papkoff protocol (Papkoff *et al.* 1965) designed with differential ethanol extractions provided to separate both different sized forms and a single Sephacryl S-200 chromatography gel filtration (Panchal and Muralidhar 2008). The selected fractions after S-200 gel filtration showed more than 95% size homogeneity of buPRL as determined by 15% SDS-PAGE and densitometry (supplementary figure 1A and B).

The purified buPRL monomer, intact form, was confirmed to be free from protease, especially from acidic protease treatment. The intact buPRL was incubated with distillated water and 20 mM citrate/phosphate buffer including salt (i.e. pH 3.0) at 37°C, respectively, and then analysed by electrophoresis at frequent intervals. When the intact buPRL was incubated in distillated water for 6 h, no lower-sized fragments were detected in SDS-PAGE either under non-reducing or reducing conditions (supplementary figure 1C–F). However, when the intact buPRL was incubated under the acidic conditions, a lower-sized form, approximately 21 kDa, was observed in SDS-PAGE under reducing conditions (supplementary figure 1F). The lower form did not significantly increase in type and quantity during the incubation time, up to 12 h.

3.2 *Proteolysis buPRL*

Protease-free intact buPRL was incubated with bovine spleen CD (the ratio of substrate vs enzyme=100:1) in acidic condition (pH 3.0) at 37°C, and then the productive mixture was separated by a 15% gel of SDS-PAGE under reducing conditions (figure 1A). Results indicated that the intact buPRL was cleaved by CD at pH 3.0 and the molecular weight of cleaved peptides were approximately 18.39 kDa (18K), 14 kDa (14K), 11.16 kDa (11K) and 7.47 kDa (7K). These sizes were identified by immunological analysis using buPRL antiserum (figure 1B). The mixture did not show a significant contamination of CD (42.12 kDa and 29 kDa) (figure 1A). This enzymatic cleavage was confirmed when in the presence of pepstatin A (Marks *et al.* 1973), a known acidic protease inhibitor, CD did not generate lower-sized peptides (figure 1C).

Analysis of the buPRL peptides by CD on 15% SDS-PAGE indicates a time-dependent enzymatic proteolysis (figure 1D and E). Under non-reducing conditions, the quantity and number of the lower-sized forms increased in a time-dependent manner (figure 1D), but under reducing conditions, the forms showed only major three different sized bands (figure 1E), and the band intensity of intact PRL decreased. In 6 h, the band intensity of cleaved isoforms decreased under non-reducing conditions as well as reducing conditions. New lowest-sized bands appeared (figure 1D and E). The acidic hydrolysed form was detected under both conditions, and its location changed from in between the cleaved form and monomer under non-reducing conditions to just below monomer under reducing conditions (figure 1D and E, L1). The amount of cleaved isoform under non-reducing condition decreased at 6 h incubation (figure 1D, L6).

3.3 *Antiangiogenic activity of buPRL-derived peptide fragments I: The enzymatic cleavage fragments mixture including intact buPRL*

Cell migration analysis by wound healing assay was performed in EAhy926. The cell line expresses factor VIII-related antigen and has the same morphological distribution as primary endothelial cells with a doubling time of 12 h (Edgell *et al.* 1983).

A dose-dependent (3.3 pg/mL to 330 µg/mL) inhibition by buPRL peptide mixture including intact form on migration of EAhy926 cells was observed (supplementary figure 2A). The effect was observed over a range of dose from 33 pg/mL to 330 pg/mL.

Hence, 33 pg/mL of the peptide mixture was used for early stage (on the day 4) CAM assay, one of the *ex vivo* methods to study angiogenesis (Ribatti *et al.* 1996) (supplementary figure 2B). The blood vessel generation reduced with the dose of the peptide mixture in a time-dependent fashion.

3.4 *Antiangiogenic activity of buPRL-derived peptide fragments II: FPLC chromatography unbound fraction*

Unbound fractions 1, 2, 3 and 4, and bound forms (fraction 5 and 6) appeared in the form of many protein peaks (figure 2A). Fractions, each 1 mL, were collected. The flow rate was 1 mL/min. The absorbance of these fractions was detected at 280 nm. The bound fractions, peak no. 5 and 6, eluted with 1 M NaCl represented buPRL monomer (data not shown). Peak no. 2 was identified by immunoreactive assay with buPRL antiserum (data not shown) and had cleaved buPRL fragments (figure 2B). This fraction was desalted by 1 K cut-off centrifugal device and lyophilized. It was then used for antiangiogenic studies.

Thirty-three pg/mL of the FPLC unbound fraction was incubated on the CAM vessels (figure 2C). The vessel

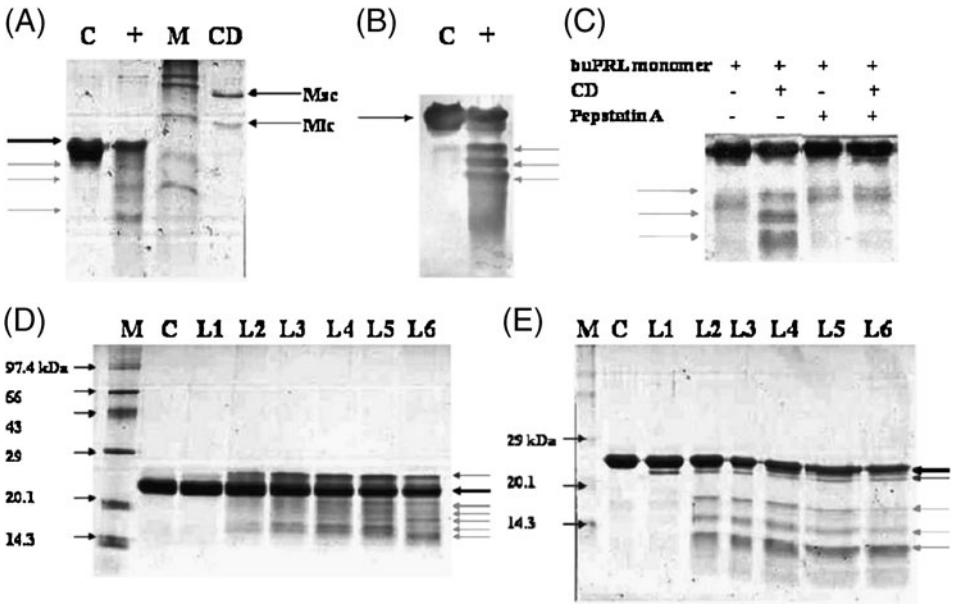

Figure 1. (**A**) Results of SDS-PAGE analysis after colloidal Coomassie blue staining. Lane C, buPRL monomer (5 μg); Lane +, buPRL monomer (5 μg) incubated with CD; Lane M, molecular weight marker; Lane CD, cathepsin D (7.49 μg); Msc, mature single chain (42.12 kDa); Mlc, mature large chain (29 kDa). (**B**) Immunoblot of **A** with anti-buPRL serum indicating the cleaved fragments of buPRL by CD. (**C**) Effect of pepstatin A on buPRL cleavage by CD. (**D**) Time course of action by CD on buPRL monomer. L1–L6 represent analysis of reaction mixture by SDS-PAGE under non-reducing conditions after 0 and 30 min, and 1, 2, 3 and 6 h, respectively. Lane C is the control where no enzyme was added; Lane M represents marker. (**E**) Same as **D** except that the gel was run under the reducing conditions.

length, volume and the number of vessel junction affected by the FPLC unbound fraction was measured using Angioquant software. The fraction significantly inhibited the vessel growth compared with the control group.

In order to understand the possible mechanism of action, NO production under 33 pg/mL of the FPLC unbound fraction treatment was measured using DAF-FM assay technique (Kojima *et al.* 1998). The NO production induced by VEGF and BK in EAhy926 cell line was inhibited by the peptides, while the peptide was unable to block Ach driven NO production (figure 2D). The buPRL peptides were more efficient in blocking BK-stimulated NO production than VEGF-stimulated NO production. For the analysis, each factor was treated with its own working concentrations to produce NO: 10 ng/mL of VEGF, 1.24 μg/mL of BK and 1.46 μg/mL of Ach.

3.5 *Antiangiogenic activity of buPRL-derived peptide fragments III: 14K buPRL*

To know which of the peptides has the antiangiogenic effect, the peptide mixture was separated on a 15% gel by SDS-PAGE under reducing and non-reducing conditions. The gel slices of 18K, 17K–15K (non-reducing condition), 14K and 11K bands were checked with CAM assay. The assay results showed that 18K and 14K under both conditions (i.e. reduced and non-reduced) had the anti-angiogenic action. The 11K, however, did not show activity when not reduced (data not shown).

For the antiangiogenic study of 14K buPRL, the sized peptides were eluted from the SDS-PAGE gel under reducing conditions with the elution buffer (20 mM Tris-HCl/0.1% SDS), and then desalted and lyophilized. The prepared 14K was tested on EAhy926 cell line. The result of the cell migration study by wound healing assay indicated that 14K peptides were working at pg/mL range (10 to 100 pg/mL). At 14K concentration of 10 pg/mL, approximately 10% and 15% inhibition in cell migration at 24 and 48 h, respectively, was observed (figure 3A). Moreover, 14K-inhibited endothelial migrations was stimulated by VEGF and BK (figure 3B and C).

Analysis of NO production by DAF-FM methods indicated that 14 K (10 pg/mL) reduced NO production in EAhy926 cell line (Data not shown), and inhibited the NO generation induced by VEGF (30 ng/mL) and BK (1.24 ug/mL), respectively (figure 3E). In the inhibition of NO production, pictogram level of 14K had a considerable effect.

3.6 *In silico study of buPRL*

To explore a structurally and functionally important motif of lower-sized fragments in exerting antiangiogenic action, the

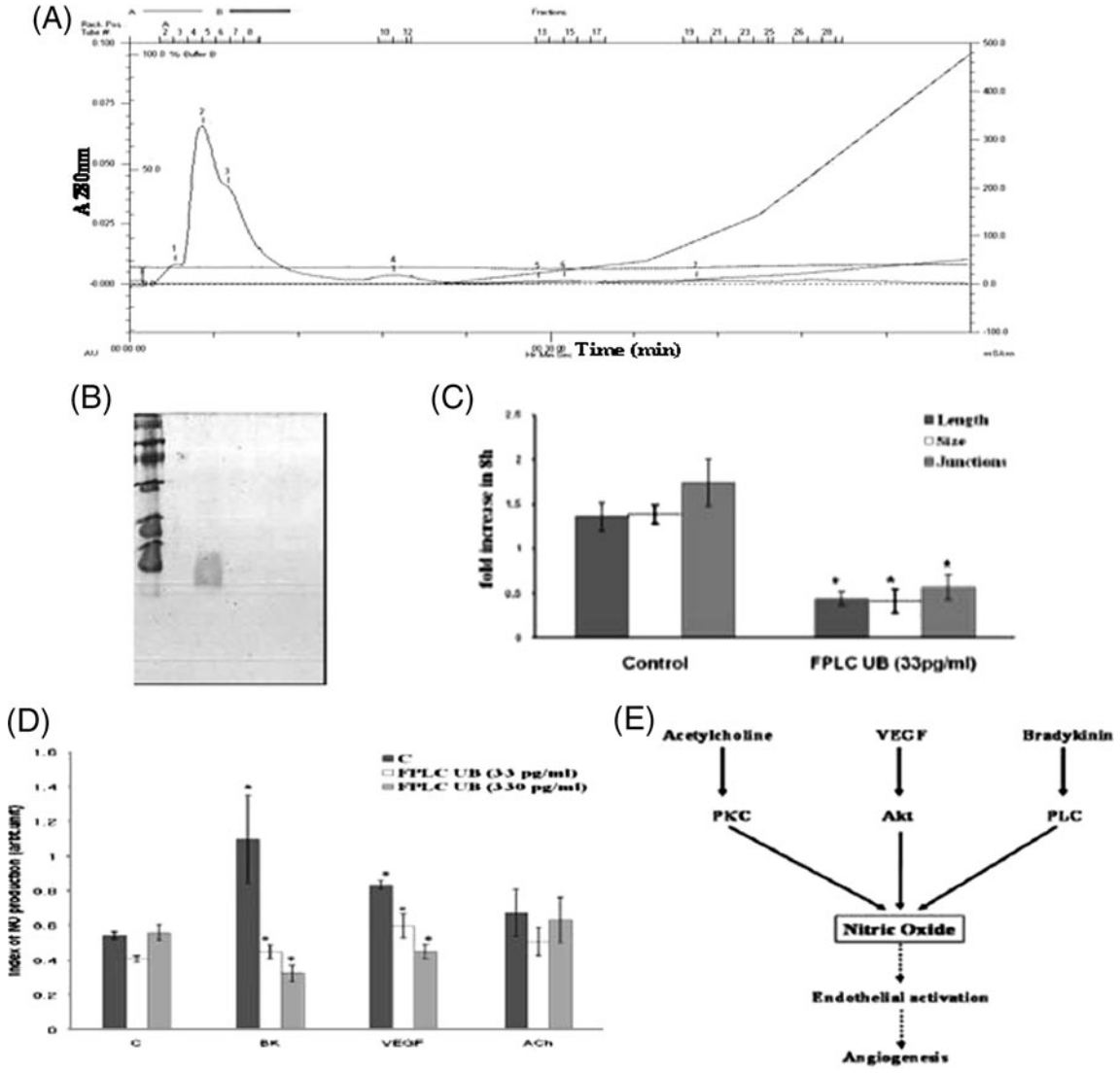

Figure 2. (**A**) FPLC profile of peptide mixture obtained after CD cleavage of buPRL. (**B**) SDS-PAGE analysis under reducing conditions of fractions 1, 2 and 3 of **A**. (**C**) CAM assay analysis of the pooled FPLC unbound fractions (33 pg/mL) using 'AngioQuant'. (**D**) Effects of the varying concentration of FPLC unbound fractions (0, 33 and 333 pg/mL) on BK, VEGF or Ach-induced NO production in EAhy926 cell line. Values are means±SEM. *Significantly different from the respective positive control at $P<0.05$. (**E**) A schematic of the role of NO in angiogenesis.

structure of the lower-sized fragment was modelled. The structure of intact buPRL was built with the template based on human PRL, 1n9dA (Keeler *et al.* 2003), by SWISS-MODEL homology modelling programme (Schwede *et al.* 2003; Arnold *et al.* 2006) (figure 4A). ABY67078 (figure 4D) was used for the prediction. The predicted structure had 74.242% sequence identity to the template and 3.31e−87 expected value (E-value). N-terminal started from blue loop structure and C-terminal ended with the red loop structure (figure 4A).

With the concept that only the N-terminal 16K peptide in human PRL has the antiangiogenic effect (Ferrara *et al.* 1991; Clapp *et al.* 1993; Khurana *et al.* 1999b), the tertiary structure of 14K (Thr1-Met132) buPRL was predicted from N-terminal amino acid sequence (figure 4B). The 14K buPRL structure (71.429% sequence identity and 1.60e−60 E-value) consisted of two and a half α-helixes.

In order to narrow down further in the motif in N-terminal fragment which has an antiangiogenic effect,

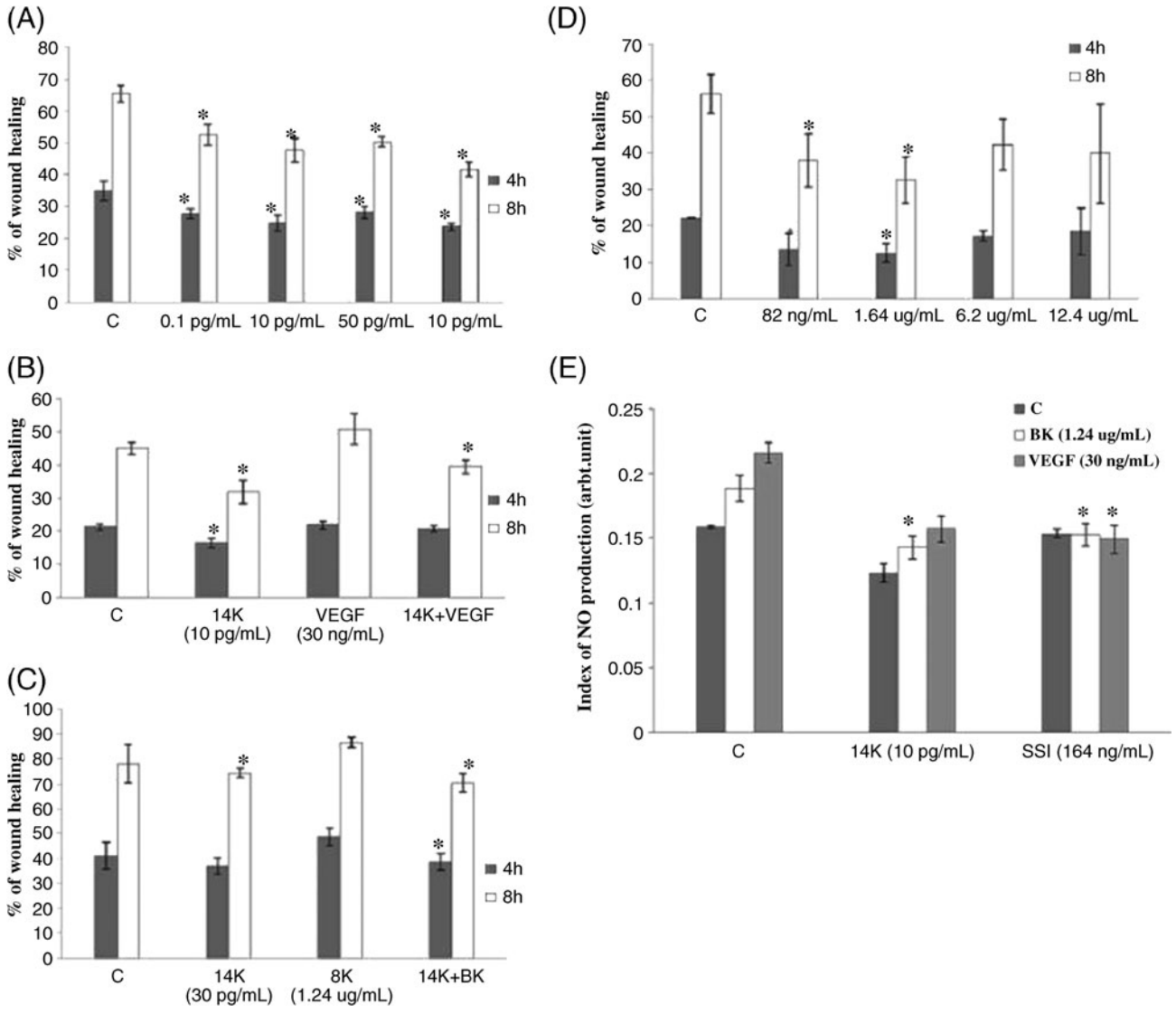

Figure 3. Results of wound healing assay (cell migration assay) in EAhy926 cell line. (**A**) Effect of 14K fragments at different doses measured at 4 and 8 h. (**B**) Effect of 14K peptides (10 pg/mL) combined with VEGF (30 pg/mL). (**C**) Effect of 14K peptides combined with BK (1.24 μg/mL). (**D**) Dose-dependent effect of SST on NO production in EAhy926 cell line. (**E**) Inhibition of BK- or VEGF-stimulated NO production by 14K (10 pg/mL) and SST (164 ng/mL). Values are means±SEM. *Significantly different from controls at $P<0.05$.

alignments between ABY67078 and some known anti-angiogenic factors like human somatostatin (hSST) (Florio *et al.* 2003) were performed with the 'protein tools' in Biology WorkBench 3.2. The alignment with hSST showed 35.71% sequence identity among the 14 residues shown in figure 4. This area, Ala45-Gln46-Gly47-Lys48-Gly49-Phe50-Ile51-Thr52-Met53-Ala54-Leu55-Asn56-Ser57-Cys58 (figure 4D), was located in the initial second loop, after the first α-helix (figure 4). This area in the predicted 14K structure was placed at the open environment (figure 4B), but not in intact PRL (figure 4A). This SST-matching sequence was commercially synthesized to study its antiangiogenic action.

3.7 *Antiangiogenic activity of buPRL derived peptide fragments III: Comparison to SST, antiangiogenic peptide*

For comparative study between buPRL fragment and hSST in the antiangiogenic action, NO production analysis (figure 3E) and CAM assay with both factors were performed (figure 5). The inhibitory effect of cell migration by SST appeared in the concentration range of 86 ng/mL to

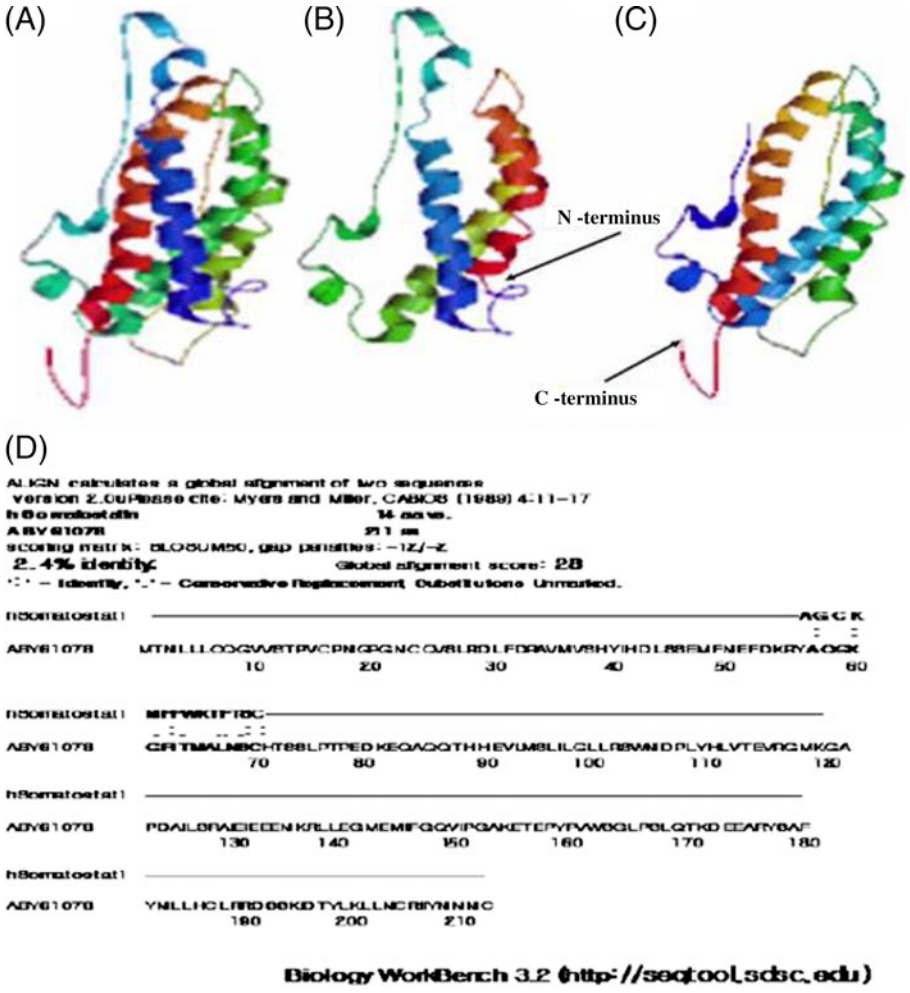

Figure 4. Tertiary structures of buPRL built by SWISS MODEL. (**A**) Tight four α-helices and loops of intact buPRL (GeneBank accession number: ABY61078) in SWISS-Pdb viewer 4.0. (**B**) Buffalo N-terminal 14K peptide (Thr1-Met132). (**C**) Human C-terminal 16K (Ala54-Cyc199). (**D**) Results of alignment of the amino acid sequence of bu PRL with that of hSST.

1.64 μg/mL. (figure 3D). 10 pg/mL (approximately 0.7 pM) of the 14K and 164 ng/mL (0.1 μM) of SST showed inhibitory effect on NO production induced by BK and VEGF (figure 3D). The inhibition of growth of vessels was also investigated in both cases. In the case of 14K eluted from the gel, even a part of the main blood vessel disappeared (figure 5A and Bi). Picogram levels of the 14K showed stronger activity than nanogram levels of SST (figures 3E, and 5A and B).

3.8 *Antiangiogenic activity of buPRL-derived peptide fragments IV: By synthetic peptide derived from buPRL*

For structure–function comparative study between buPRL and hSST on the antiangiogenic function, the synthetic peptide, Ala-Gly-Lys-Gly-Phe-Ile-Thr-Met-Ala-Leu-Asn-Ser-Cys (13 mer) (lacking Gln in the 2nd position), derived from the second loop of buPRL aligned with human SST, was used for cell migration assay, CAM assay and tube formation (figure 5B–E). The EAhy926 cells migration was inhibited at 1 pg/mL of the synthesized peptide derived from buPRL, but this phenomenon did not exhibit dose dependence (figure 5C). The vessel development in chorioallantoic membrane reduced and disappeared at even 1 pg/mL (approximately 0.7 pM) of the buPRL-derived peptide treatment (figure 5D). The antiangiogenic function of synthesized peptide was confirmed using tube formation assay. Tube formation by endothelial cells (vessel tunnel) was blocked at 1 pg/mL of the synthesized peptide treatment (figure 5E).

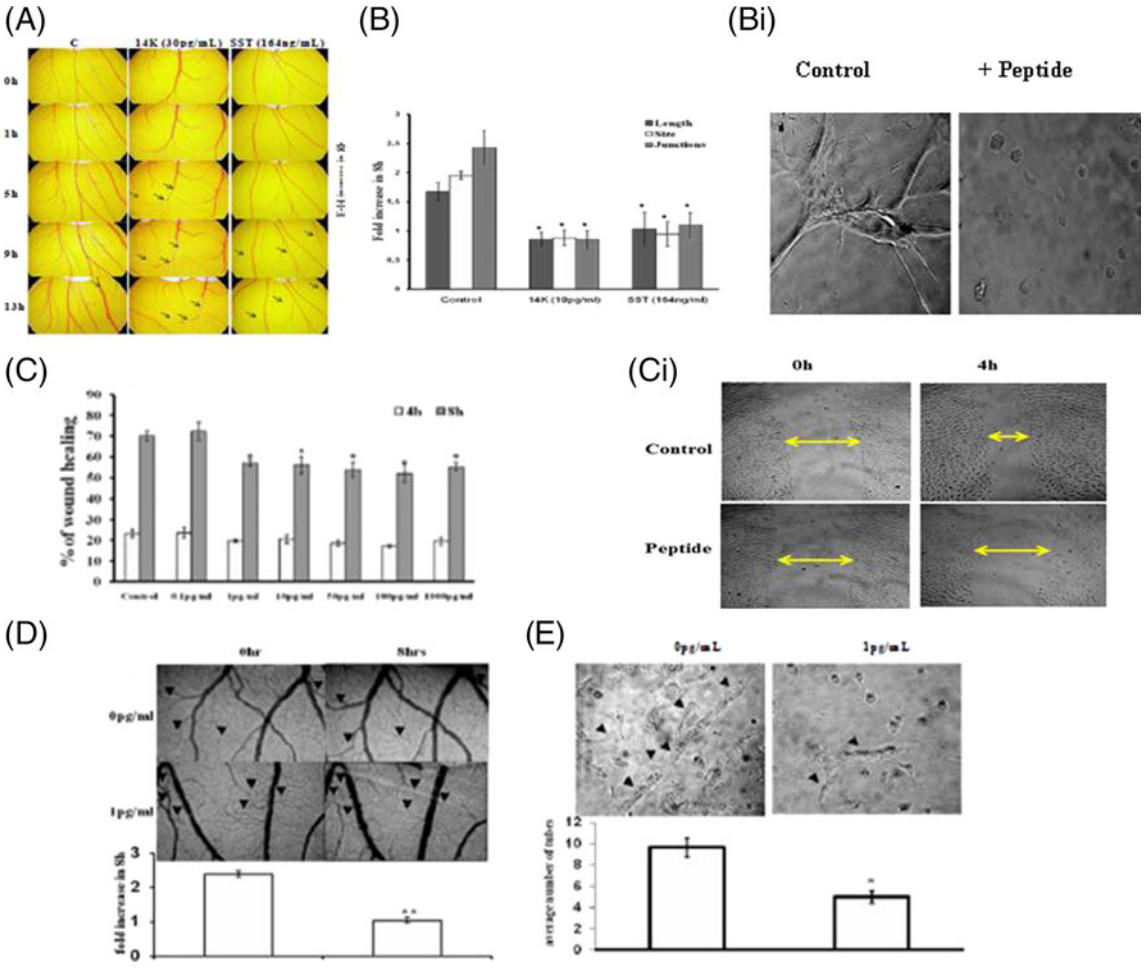

Figure 5. Results of CAM assay of 14 K and SST. (**A**) Antiangiogenic effect in time-dependent manner. (**B**) The estimation of vessel length, size and junction number. The Antiangiogenic activity by the synthesized peptide derived from buPRL. (**C**) Cell migration by wound healing assay. (**D**) CAM assay. (**E**) Tube formation assay. Values are means±SEM. *Significantly different from controls $P<0.05$. **$P<0.01$. Appropriate actual photographs are indicated as **Bi** and **Ci**.

4. Discussion

When incubated with acidic buffer, the buPRL monomer generated a 21K fragment but there was no time-dependent increase in the concentration of the 21K fragment, indicating that this fragment arose as a result of hydrolysis of a disulfide loop either at the N-terminal or at the C-terminal and not due to nicking of peptide bond (supplementary figure 1E and F). This proves that the purified intact buPRL was protease free, especially acid protease, and therefore would be an ideal candidate for use in proteolysis studies. In the present study, the cleaved isoform with a nick in the large disulphide loop (Mittra 1980b) seemed to produce 18K and 7K or 14K and 7K by reduction. Moreover, the cleavage action of the endosomal acidic enzyme, CD, may have a recognition pattern at the cleavage site in the amino acid sequence of buPRL.

The sizes of buPRL fragments obtained by CD are different from the sizes of cleaved fragments of PRL from other species: rat pituitary (16K and 8K) (Mittra 1980a, b), mouse pituitary (16K and 8K) (Sinha and Gilligan 1984), and human pituitary (17K, 16.5K, 15K, 11K, 8K and 5K) (Piwinica *et al.* 2006) PRL (figure 6A). These different patterns of cleavage could be due to micro-variation in the primary structure among species. Comparing the cleaved sequences between human and rat PRLs, Tyr147-Pro148-Val149-Trp150-Ser151 of human and Tyr145-Leu146-Val147-Trp148-Ser149 of rat are homologous (Piwinica *et al.* 2006) (figure 6B). The presence of Pro148 and Leu132 controlled the cleavage pattern in hPRL (Piwinica

et al. 2006). Pro148 prevented high cleavage efficiency at 147–148 and 150–151 sites, while Leu132 produced the additional cleavage at 132–133 sites (Piwinica *et al.* 2006). Buffalo PRL sequence has the same sequence at 147–151 sites as in hPRL, but not at residue 132 site (figure 6B). The Pro148 in buPRL also seems to link to a specific cleavage pattern. Hence, 18K and 14K of buPRL were considered homologous to 17K and 15K of hPRL, respectively. We could not detect a fragment similar to the 16.5K fragment of hPRL.

Angiogenesis, the process of developing new blood vessels from preexisting vessels, is crucial to reproduction, growth and wound healing (Folkman and Shing 1992). In the last two decades, numerous studies reported novel angiogenic regulators (Iyer and Acharya 2002). Among the angiogenic regulators, PRL fragment is one of the very paradoxical molecules. Its intact form has pro-angiogenic action (Struman *et al.* 1999), inducing cell proliferation and motility, and relates to breast carcinogenesis (Clevenger *et al.* 2003). The PRL fragments as well as intact PRL were are also known to be secreted from vascular endothelial cells (Ochoa *et al.* 2001). The antiangiogenic and anti-mitogenic effects of peptide fragments were observed in BBBE and HUVE cells, respectively, by incubating them with PRL antibody, which suggested the possibility that they act as autocrine regulators of angiogenesis, (Clapp *et al.* 1998; Corbacho *et al.* 2000).

In the present study, the antiangiogenic activity of buPRL-derived peptides was demonstrated *in vitro* and *ex vivo*. Endothelial cell migration is fundamental to angiogenesis (Lamalice *et al.* 2007), because endothelial cells, derived from mesodermal cells, form capillary blood and lymphatic vessels (Venes and Thomas 2001). Earlier reports found antiangiogenic activity of r16K (Ferrara *et al.* 1991) and recombinant h16K (Clapp *et al.* 1993; D'Angelo *et al.* 1999) in nanomalar concentrations. The present study demonstrates that buPRL-derived peptides have an anti-angiogenic activity in picomolar concentration. Even the cleaved fragments mixed with intact buPRL, considered a pro-angiogenic factor (Struman *et al.* 1999), are effective at

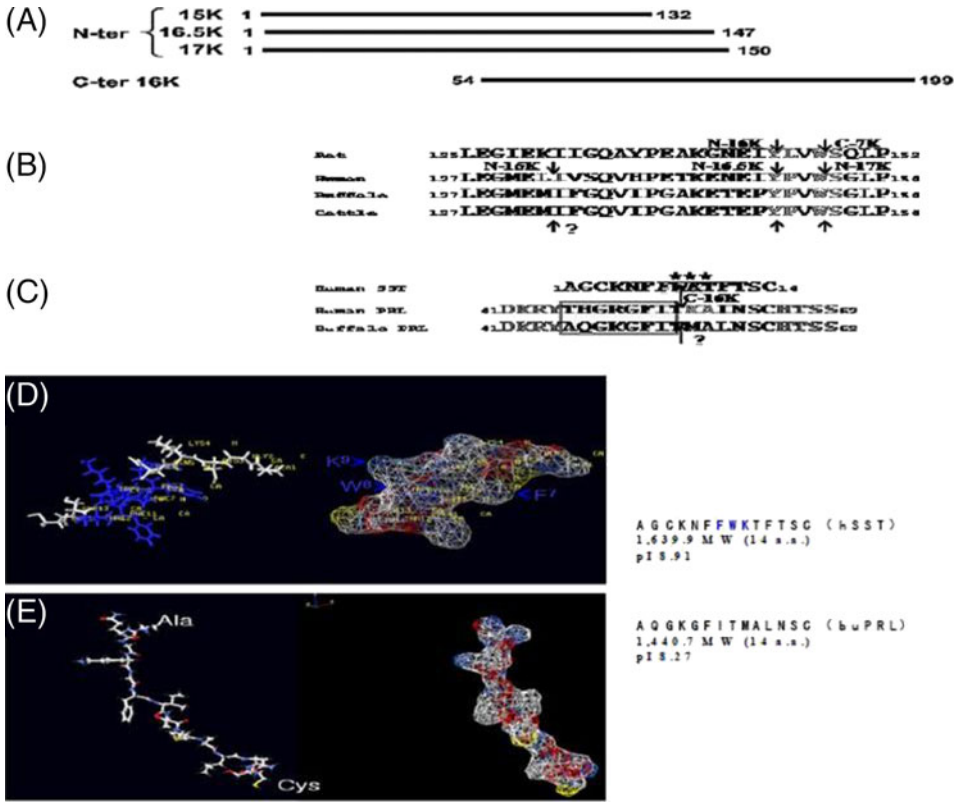

Figure 6. CD and thrombin cleavage site in the primary sequences of rat, human, buffalo and cattle PRLs. (**A**) In human PRL three N-termini by CD and C-terminus by thrombin (figure from Piwnica, *et al.* 2004). (**B**) CD cleavage sites in rat, human, buffalo and cattle PRLs. (**C**) The SST aligned sequences of buPRL and buGH are partially or completely involved in the sequence of N-terminus fragment known as antiangiogenic factor. Triple * in hSST is the specific binding site to SSTRs. The square window indicates the considered sequence has an antiangiogenic action. Arrows indicate the cleavage sites. (**D**) hSST in SWISS-Pdb viewer 4.0. Blue arrows and alphabets represent SST receptor binding sites. (**E**) The synthetic peptide derived from buPRL..Molecular size and pI of each peptide were gained from ExPASy Proteomics tools.

the lower concentration level (supplementary figure 2). The results of our study prove that buPRL peptides cleaved by CD have the antiangiogenic action, and these negative factors for angiogenesis should be N-terminal peptides. These peptides inhibited NO production and hence NO-mediated angiogenesis stimulated by VEGF or BK.

NO, produced by NO synthase (NOS), is a second messenger in the regulation of physiological and patho-physiological process in the cardiovascular, nervous and immune systems (Moncada and Higgs 1993; Nathan and Xie 1994). NO is involved in cell migration and cell protection (Lee *et al.* 2005; Kolluru *et al.* 2007). NO-mediated pathway is a well known signalling mechanism of angiogenesis, vasopermeability and vasorelaxation in relation to VEGF (Ferreira and Henzel 1989; Ishikawa *et al.* 1989), BK (Regoli and Barabe 1980; Ferreira *et al.* 1992) and Ach (Palmer *et al.* 1989) actions (figure 2E). Gonzalez *et al.* (2004) reported that human and rat 16K PRL fragments inhibited NOS activation induced not only by VEGF and BK but also by Ach, in endothelial cells. Buffalo PRL fragments seem not to be correlated to the pathway stimulated by Ach in EAhy926 (figure 2D). Moreover, the buPRL peptides were more effective in inhibiting the BK-mediated NO mechanism than that by VEGF (figure 2D). It is not known, however, how this peptide blocks the NO pathway. We envisage two possible mechanisms. One is that the peptides act as receptor antagonists of angiogenic factors, and the other is that the peptides induce another pathway to inhibit NO production driven by these angiogenic factors. Besides, the role of individual amino acid residues in the antiangiogenic action is not yet clear.

Generally, the conformation of the cleaved fragment is either new and unstable or native-like which is less stable than that of the original (Creighton 1993). No experimental details are available on the conformation of the cleaved fragment. Nevertheless, a significant difference in the N-terminal 14K PRL structure from the intact PRL was that the loop between the first and the second α-helices were loosened and more opened to the environment. In the intact form, the loop was close to the fourth α-helix (figure 4A). The disulfide bond between the loop and the fourth α-helix, between Cys58 and Cys174, in the centre of the loop might be giving more compact configuration.

Somatostatin, a small peptide (14 amino acids) secreted from hypothalamus, is a negative regulator of growth hormone (GH) release (Norman 1997). Widely distributed throughout the body, SST binds to five different subtypes of its cognate receptors (SSTR1-5), one of them being a G-protein-coupled receptor present on the cell membrane (Patel *et al.* 1990; Lahlou *et al.* 2004). While the five SSTRs bind the natural peptide, SSTR2, SSTR3, and SSTR5 can bind its synthetic analogues (Lahlou *et al.* 2004). SST and its analogues inhibit angiogenesis and also the production and secretion of angiogenic factors including VEGF (Barrie *et al.* 1993). It was reported that SST blocked Kaposi sarcoma (KS) cells (KS-Imm), isolated from a kidney-transplanted, immuno-suppressed patient and also highly angiogenic, xenografts into nude (nu/nu) mice through angiostasis (Albini *et al.* 1999). SST also induced cell death of human somatotrph tumor cells (SSTR2) (Ferrante *et al.* 2006). In the study with vascular endothelial cell (dominated by SSTR3; Reisine and Bell 1995), SST inhibited cell proliferation through blocking of both endothelial NOS (eNOS) and MAPK activations. SST is a powerful anti-tumour angio-static agent. The results of the present work (figures 3, 6A and 6B) confirm that SST and 14K buPRL are significant antiangiogenic factors, and 14K is more effective than SST in the antiangiogenesis assays. The antiangiogenesis brought about by buPRL fragment seems to be related to the inhibition of vasopermeability of endothelial cells (figure 2D).

Small ligands tend to bind, relatively speaking, the interior of globular proteins, while linear ligands tend to bind in clefts on the surface of proteins (Creighton 1993). The small and linear structure of the synthesized peptide (figure 6E) enables it to bind to both the interior of putative receptors and to the clefts on the surface of receptors. The synthetic peptide, Ala45-Gly47-Lys48-Gly49-Phe50-Ile51-Thr52-Met53-Ala54-Leu55-Asn56-Ser57-Cys58, also showed more active than SST in the antiangiogenic action. This SST-matching sequence peptide had a structure (linear) different from SST, which had α-helix structure (figure 6D). This active motif for antiangiogenesis is not involved in binding to the PRLR sites, especially the second half of loop 1 (His59, Pro66 and Lys69) of site 1 (Goffin *et al.* 1992). This result also demonstrates that Ala45 to Met53 can be the active sites for angiostatic function. The C-terminal 16K peptide (54–199 residues) of hPRL does not appear to have the function of antiangiogenesis (Khurana *et al.* 1999b) (figure 6A). However, in the C-terminal 16K fragment of hPRL, the fourth helix is still close to the partial second loop, which becomes exposed to environment in the N-terminal 16K fragment of hPRL (figure 4B and C). Because of this, the C-terminal 16K fragment of hPRL may not have antiangiogenic action.

Three residues, Phe7-Trp8-Lys9, in SST sequence appear to have the crucial role in binding with high affinity to all SST receptors, SSTR1 to SSTR5 (Poitout *et al.* 2001). However, in the synthetic sequence derived from buPRL, Ala1-Gln2-Gly3-Lys4-Gly5-Phe6-Ile7-Thr8-Met9-Ala10-Leu11-Asn12-Ser13-Cys14, 'Ile7-Thr8-Met9' is found instead of 'Phe7-Trp8-Lys9'. In the SST-matching sequence of hPRL, 'Ile51-Thr52-Lys53' replaces the SST tri-peptide sequence ('Phe7-Trp8-Lys9') positions (figure 6C). This leads to the question of whether buPRL fragments bind to SSTR3 or not, and if the fragments bind to SSTR3, which residues in the sequence of the

fragments bind to the receptor and mediate the antiangiogenic action. In the PRL fragments- and SST-mediated inhibition of the angiogenesis, there are similar mechanistic patterns. Both factors blocked VEGF-induced cell proliferation, which is known to be through the MAPK pathway in vascular endothelial cells (D'Angelo *et al.* 1999).

The hPRL and hGH tilted peptides (14-amino-acid sequence) consisting of 9 hydrophobic amino acids induce endothelial cell apoptosis and inhibit endothelial cell proliferation and capillary formation (Nguyen *et al.* 2006). The tilted peptide has been known to destabilize membrane and lipid core and is characterized by an asymmetric distribution of hydrophobic residues along the axis when helical. However, the synthetic tilted peptides derived from hPRL and hGH show 4 times and 32 times less activity, respectively, than the 16K hPRL *in vitro* (Nguyen *et al.* 2006). The synthetic peptide related to buPRL represents differences in structure and functional sensitivity from those of the tilted peptides. This peptide has similar sensitivity with 14K buPRL in the inhibition of angiogenesis *in vitro* and *ex vivo*. Although the peptide includes 9 hydrophobic amino acids, it does not form a helix (figure 6E). These differences imply that the synthetic peptide related to buPRL has a receptor-binding mediated antiangiogenic function, rather than protein-membrane-interaction-mediated function.

The present study suggests that buPRL gives upon cathepsin digestion a 16K-like fragment, but of 14K size and more cleaved fragments in buPRL, which have an antiangiogenic action. The antiangiogenic action of the fragments is, at least, related to the initial part of the sequence of the second loop between first and second α-helices. Furthermore, the synthetic peptide (derived by hSST matching area of buPRL) can be a potential anticancer therapeutic agent as well as for treatment of vascular, rheumatoid and other diseases whose etiology necessarily involves angiogenesis (Folkman 1995). Confirming the relevance of this idea requires demonstrating whether the buPRL fragments have N-terminal structure, and whether there are other sequences between Thr1-Tyr44 having antiangiogenic action. Further work is required to explore whether SSTR3 is the specific receptor for 14K and other cleaved peptides, and if not, what is the specific receptor to the peptides, and what sequence part plays a crucial role in this antiangiogenic action?

Acknowledgements

The financial assistance provided by Indian Council of Cultural Relations and University of Delhi through 'R&D Doctoral Research Programme' support scheme is highly acknowledged.

References

Albini A, Florio T, Giunciuglio D, Masiello L, Carlone S, Corsaro A, Thellung S, Cai T, Noonan DM and Schettini G 1999 Somatostatin controls Kaposi's sarcoma tumor growth through inhibition of angiogenesis. *FASEB J.* **13** 647–655

Arnold K, Bordoli L and Kopp JT 2006 The SWISS-MODEL workspace: a web-based environment for protein structure homology modeling. *Bioinformatics* **22** 195–201

Baldocchi RA, Tan L, King DS and Nicoll CS 1993 Mass spectrometric analysis of the fragments produced by cleavage and reduction of rat prolactin: Evidence that the cleaving enzyme is cathepsin D. *Endocrinology* **133** 935–938

Barrie R, Woltering EA, Hajarizadeh H, Mueller C, Ure T and Fletcher WS 1993 Inhibition of angiogenesis by somatostatin and somatostatin-like compounds is structurally dependent. *J. Surg. Res.* **55** 446–450

Bradford MM 1976 A rapid and sensitive method for the quantitation of microgram quantities of protein utilizing the principle of protein-dye binding. *Anal. Biochem.* **72** 248–754

Candiano G, Bruschi M, Musanta L, Santucci L, Ghiggeri GM, Carnemolla B, Orecchia P, Zardi L and Righetti PG 2004 Blue silver:A very sensitive colloidal Coomassie G-250 staining for proteome analysis. *Electrophoresis* **25** 1327–1333

Clapp C 1987 Analysis of the proteolytic cleavage of prolactin by the mammary gland and liver of the rat: Characterization of the cleaved and 16K forms. *Endocrinology* **121** 2055–2064

Clapp C, López-Gómez FJ, Nava G, Corbacho A, Torner L, Macotela Y, Dueñas Z, Ochoa A, *et al.* 1998 Expression of prolactin mRNA and of prolactin-like proteins in endothelial cells: evidence for autocrine effects. *J. Endocrinol.* **158** 137–144

Clapp C, Martial JA, Guzman RC, Rentier-Delrue F and Weiner RI 1993 The 16-kilodalton N-terminal fragment of human prolactin is a potent inhibitor of angiogenesis. *Endocrinology* **133** 1292–1299

Clevenger CV, Furth PA, Hankinson SE and Schuler LA 2003 The role of prolactin in mammary carcinoma. *Endocr. Rev.* **24** 1–27

Corbacho AM, Macotela Y, Nava G, Torner L, Dueñas Z, Noris G, Morales MA, de la Escalera M and Clapp C 2000 Human umbilical vein endothelial cells express multiple prolactin isoforms. *J. Endocrinol.* **166** 53–62

Creighton TE 1993 The folded conformations of globular proteins; in *Proteins structures and molecular properties* (ed) TE Creighton (New York: WH Freeman and Company) pp. 201–260

D'Angelo G, Martini J-F, Iiri T, Fantl WJ, Martial J and Weiner RI 1999 16K human prolactin inhibits vascular endothelial growth factor-induced activation of Ras in capillary endothelial cells. *Mol. Endocrinol.* **13** 692–704

Edgell C-JS, McDonald CC and Graham JE 1983 Permanent cell line expressing human factor VII-related antigen established by hybridization. *Proc. Natl. Acad. Sci. USA* **80** 3734–3737

Ferrante E, Pellegrini C, Bondioni S, Peverelli E, Locatelli M, Gelmini P, Luciani P, Peri A, *et al.* 2006 Octreotide promotes apoptosis in human somatotroph tumor cells by activating somatostatin receptor type 2. *Endocr. Relat. Cancer* **13** 955–962

Ferrara N, Clapp C and Weiner R 1991 The 16K fragment of prolactin specifically inhibits basal or fibroblast growth factor stimulated growth of capillary endothelial cells. *Endocrinology* **129** 896–900

Ferreira MA, Andrade SP, Pesquero JL, Feitosa MH, Oliveira GM, Rogana E, Nogueira JC and Beraldo WT 1992 Kallikrein-kinin system in the angiogenesis. *Agents Actions Suppl.* **38** 165–174

Ferreira N and Henzel WJ 1989 Pituitary follicular cells secrete a novel heparin-binding growth factor specific for vascular endothelial cells. *Biochem. Biophys. Res. Commun.* **161** 851–858

Florio T, Villa MV, Corsaro AA, Thellung CS, Culler MD, Pfeffer U, Noonan DM, Schettini G and Albini A 2003 Somatostatin inhibitors tumor angiogenesis and growth via somatostatin receptor-3-mediated regulation of endothelial nitric oxide synthesis and mitogen-activate protein kinase activities. *Endocrinology* **144** 1574–1584

Folkman J 1995 Angiogenesis in cancer, vascular, rheumatoid and other disease. *Nat. Med.* **1** 27–31

Folkman J and Shing Y 1992 Angiogenesis. *J. Biol. Chem.* **267** 10931–10934

Gasteriger E, Hoogland C, Gattiker A, Duvaud S, Wilkins MR, Appel RD and Bairoch A 2005 Protein identification and analysis tools on the ExPASy server; in *The proteomics protocols handbook* (eds) JM Walker (New Jersey: Humana Press Inc) pp. 571–607

Goffin V, Norman M and Martial JA 1992 Alanine-scanning mutagenesis of human prolactin: importance of the 58–74 region for bioactivity. *Mol. Endocrinol.* **6** 1381–1392

Gonzalez C, Corbacho AM, Eiserich JP, Garcia C, Lopez-Barrera F, Morales-Tlalpan V, Barajas-Espinosa A, Diaz-Munoz M, *et al.* 2004 16K-prolactin inhibits activation of endothelial nitric oxide synthase, intracellular calcium mobilization and endothelium-dependent vasorelazation. *Endocrinology* **10** 1210

Guex N and Peitsch MC 1997 SWISS-MODEL and the Swiss-PdbViewer: An environment for comparative protein modeling. *Electrophoresis* **18** 2714–2723

Harrington MG 1990 Elution of protein from gels. *Method Enzymol.* **182** 488–495

Ishikawa F, Miyazone K, Hellman U, Drexler H, Wernstedt C, Hagiwara K, Usuki K, Takaku F, Risau W and Heldin CH 1989 Identification of angiogenic activity and the cloning and expression of platelet-derived endothelial cell growth factor. *Nature (London)* **338** 557–562

Iyer S and Acharya KR 2002 Angiogenesis: What we know and do not know. *Proc. Indian Nat. Sci. Acad.* **B68** 415–478

Keeler C, Dannies PS and Hodsdon ME 2003 The tertiary structure and backbone dynamics of human prolactin. *J. Mol. Biol.* **328** 1105–1121

Khurana S, Kuns R and Ben-Jonathan N 1999a Heparin-binding property of human prolactin: A novel aspect of prolactin biology. *Endocrinology* **140** 1026–1029

Khurana S, Liby K, Buckley AR and Ben-Jonathan N 1999b Proteolysis of human prolactin: Resistance to cathepsin D and formation of a nonangiostatic, C-terminal 16K fragment by thrombin. *Endocrinology* **140** 4127–4132

Kojima H, Nakatsubo N, Kikuchi K, Kawahara S, Kirino Y, Nagoshi H, Hirata Y and Nagano T 1998 Detection and imaging of nitric oxide with novel fluorescent indicators: diaminofluoresceins. *Anal. Chem.* **70** 2446–2456

Kolluru GK, Tamilarasan KP, Rajkumar AS *et al.* 2007 Nitric oxide/cGMP protects endothelial cells from hypoxia-mediated leakiness. *Eur. J. Cell Biol.* 1–15

Laemmli UK 1970 Cleavage of structure proteins during the assembly of the head of bacteriophage T4. *Nature (London)* **227** 680–685

Lahlou H, Guillermet J, Hortala M, Vernejoul F, Pyronnet S, Bousquet C and Susini C 2004 Molecular signaling of somatostatin receptors. *Ann. N.Y. Acad. Sci.* **1014** 121–131

Lamalice L, Boeuf FL and Huot J 2007 Endothelial cell migration during angiogenesis. *Circ. Res.* **100** 782–794

Lee JS, Decker NK, Chatterjee S, Yao J, Friedman S and Shah V 2005 Mechanisms of nitric oxide interplay with Rho GTPase family members in modulation of actin membrane dynamics in pericytes and fibroblasts. *Am. J. Pathol.* **166** 1861–1870

Lkhider M, Castino R, Bouguyon E, Isidoro C and Ollivier-Bousquet M 2004 Cathepsin D released by lactating rat mammary epithelial cells is involved in prolactin cleavage under physiological conditions. *J. Cell Sci.* **117** 5155–5164

Lowry OH, Rosenbrough NJ, Farr AL and Randall RJ 1951 Protein measurement with the folin phenol reagent. *J. Biol. Chem.* **193** 265–275

Madri JA, Pratt BM and Tucker AM 1988 Phenotypic modulation of endothelial cells by transforming growth factor-β depends upon the composition and organization of the extracellular matrix. *J. Cell Biol.* **106** 1375–1384

Marks N, Grynbaum A and Lajtha A 1973 Pentapeptide (pepstatin) inhibition of brain acid protease. *Science* **181** 949–951

Mittra I 1980a A novel "cleaced PRL" in the rat pituitary: Part I biosynthesis, characterization and regulatory control. *Biochem. Biophys. Res. Commun.* **95** 1750–1759

Mittra I 1980b A novel "cleaced PRL" in the rat pituitary: Part II in vivo mammary mitogenic activity of its N-terminal 16K moiety. *Biochem. Biophys. Res. Commun.* **95** 1760–1780

Moncada S and Higgs A 1993 The L-arginine-nitric oxide pathway. *N. Engl. J. Med.* **329** 2002–2012

Nathan C and Xie Q 1994 Nitric oxide synthase: roles, tolls, and controls. *Cell* **78** 915–918

Nguyen NQN, Tabruyn SP, Lins L, Lion M, Cornet AM, Lair F, Rentier-Delrue F, Brasseur R, Martial JA and Struman I 2006 Prolactin/growth hormone-derived antiangiogenic peptides highlight a potential role of tilted peptides in angiogenesis. *Proc. Natl. Acad. Sci. USA* **103** 14319–14324

Nicoll CS 1997 Cleavage of prolactin by its target organs and the possible significance of this process. *J. Mammary Gland Biol. Neoplasia* **2** 81–89

Niemisto A, Dunmire V, Yli-Harja O, Zhang W and Shmulevich I 2005 Robust quantification of *in vitro* angiogenesis through image analysis. *IEEE Trans. Med. Imag,* **24** 549–553

Norman W 1997 *Hormone* (London: Academic press)

Ochoa A, Montes de OP, Rivera JC, Dueñas Z, Nava G, Martínez de la EG and Clapp C 2001 Expression of prolactin gene and secretion of prolactin by rat retinal capillary endothelial cells. *Invest. Ophthalmol. Visual Sci.* **42** 1639–1645

Palmer RMJ, Ferrige AG and Moncada S 1989 Nitric oxide release accounts for the biological activity of endothelium-derived relaxing factor. *Nature (London)* **327** 524–526

Panchal M and Muralidhar K 2008 Purification of monomeric prolactin charge isoform from buffalo pituitaries. *Prep. Biochem. Biotech.* **38** 94–104

Papkoff H, Gospodarowicz D, Candiotti A and Li CH 1965 Preparation of ovine interstitial cell-stimulating hormone in high yield. *Arch. Biochem. Biophys.* **111** 431–438

Patel YC, Murthy KK, Escher EE, Banville D, Spiess J and Srikant CB 1990 Mechanism of action of somatostatin: an overview of receptor function and studies of the molecular characterization and purification of somatostatin receptor proteins. *Metabolism* **39** 63–69

Piwnica D, Touraine P, Struman I, tabruyn S, Bolbach G, Clapp C, Martial JA, Kelly PA and Goffin V 2004 Cathepsin D processes human prolactin into multiple 16K-like N-terminal fragments: Study of their antiangiogenic properties and physiological relevance. *Mol. Endocrinol.* **18** 2522–2542

Piwnica D, Fernandez I, Binart N, Touraine P, Kelly PA and Goffin V 2006 A new mechanism for prolactin processing into 16K PRL by secreted cathepsin D. *Mol. Endocrinol.* **20** 3263–3278

Poitout L, Roubert P, Contour-Galcera MO, Moinet C, Lannoy J, Pommier J, Plas P, Bigg D and Thurieau C 2001 Identification of potent non-peptide somatostatin antagonists with sst3 selectivity. *J. Med. Chem.* **44** 2990–3000

Regoli D and Barabe J 1980 Pharmacology of bradykinin and related kinins. *Pharmacol. Rev.* **32** 1–46

Reisine T and Bell GI 1995 Molecular biology of somatostatin receptors. *Endocr. Rev.* **16** 427–442

Ribatti D, Vacca A, Roncali L and Dammacco F 1996 The chick embryo chorioallantoic membrane as a model for in vivo research on angiogenesis. *Int. J. Dev. Biol.* **40** 1189–1197

Schwede T, Kopp J, Guex N and Peitsc MC 2003 SWISS-MODEL: an automated protein homology-modeling server. *Nucleic Acids Res.* **31** 3381–3385

Sinha YN and Gilligan TA 1984 A cleaved form of PRL in the mouse pituitary gland: Identification and comparison of *in vitro* synthesis a release in strains with high and low incidence of mammary tumors. *Endocrinology* **114** 2046–2053

Sinha YN, Gilligan TA, Lee DW, Hollingsworth D and Markoff E 1985 Cleaved prolactin: Evidence for its occurrence in human pituitary gland and plasma. *J. Clin. Endocrinol. Metab.* **60** 239–243

Staton CA, Stribbling SM, Tazzyman S, Hughes R, Brown NJ and Lewis CE 2004 Current methods for assaying angiogenesis *in vitro* and *in vivo*. *Int. J. Exp. Pathol.* **85** 233–248

Struman I, Bentzien F, Lee H, Mainfroid V, D'Angelo G, Goffin V, Weiner RI and Martial JA 1999 Opposing actions of intact and N-terminal fragments of the human prolactin/growth hormone family members on angiogenesis: novel mechanism for the regulation of angiogenesis. *Proc. Natl. Acad. Sci. USA* **96** 1246–1251

Towbin H, Staehelin T and Gordon J 1979 Electrophoretic transfer of proteins from polyacrylamide gels to nitrocellulode sheets: procedure and some applications. *Proc. Natl. Acad. Sci. USA* **76** 4350–4354

Venes D and Thomas CL 2001 *Taber's cyclpedic medical dictionary* (London: FA Davis company)

Vogt S and Freitag R 1998 Displacement chromatography using the UNO Q continuous bed column as a stationary phase. *Biotechnol. Prog.* **14** 742–748

MS received 16 August 2010; accepted 11 April 2011

*e*Publication: 16 May 2011

Corresponding editor: MANEESHA INAMDAR